FUSE

Fungal Systematics and Evolution

VOLUME 13
JUNE 2024
PAGES 1–14

doi.org/10.3114/fuse.2024.13.01

Two novel *Pleosporales* species isolated from the bark of *Acer saccharum*

J.N. Mack[1,2], A. Sproule[1], S.W. Shields[1], K.A. Seifert[2], M. Smith[2], D.P. Overy[1,2*]

[1]Biodiversity (Mycology and Microbiology), Agriculture and Agri-Food Canada, 960 Carling Avenue, Ottawa, Ontario K1A 0C6
[2]Department of Biology, Carleton University, 125 Colonel By Drive, Ottawa, ON K1S 5B6

*Corresponding author: david.overy@AGR.GC.CA

Key words:
Coelomycetes
dilution-to-extinction
Dothideomycetes
naphthoquinones
new taxa
particle-filtration
phylogenetic analyses
pullulan

Abstract: During a survey of culturable microfungi from the bark of sugar maple (*Acer saccharum*), *Atrocalyx glutinosus* and *Nigrograna rubescens*, two novel species of *Pleosporales* (*Dothideomycetes*) were isolated from several locations in eastern Ontario, Canada. Formal species descriptions are presented based on unique colony phenotypes and micromorphological characteristics and supported using multi-locus molecular phylogenetic comparisons with similar species. Both *A. glutinosus* and *N. rubescens* produce pycnidial asexual morphs in culture. As their names imply, under specific culture conditions, *A. glutinosus* excretes large amounts of the glutinous polysaccharide pullulan and *N. rubescens* produces a dark red naphthoquinone pigment that diffuses in the culture medium.

Citation: Mack JN, Sproule A, Shields SW, Seifert KA, Smith M, Overy DP (2024). Two novel *Pleosporales* species isolated from the bark of *Acer saccharum* . *Fungal Systematics and Evolution* **13**: 1–14. doi: 10.3114/fuse.2024.13.01
Received: 8 August 2023; **Accepted:** 8 January 2024; **Effectively published online:** 7 February 2024
Corresponding editor: P.W. Crous

INTRODUCTION

The *Pleosporales* is the largest order of *Dothideomycetes*, containing, as of 2021, 88 families (Wijayawardene *et al*. 2022). Species of *Pleosporales* are found in diverse ecological niches; many occur as saprophytes or are parasites of other fungi. Sexual morphs of *Pleosporales* are perithecial with bitunicate asci and exhibit a variety of ascospore morphologies (Hongsanan *et al.* 2020). Most species have an associated asexual morph, most often phoma-like coelomycetes or hyphomycetes with dry, pigmented multi-septate or muriform conidia (Zhang *et al*. 2011). For many species, no sexual morph is known.

During our survey of culturable microfungi from the bark of the sugar maple (*Acer saccharum*), two unusual *Pleosporales* fungi were commonly isolated. Both appear to be undescribed species based on both their morphological characters and phylogenetic analyses, which placed them in the families *Lophiotremataceae* and *Nigrograna*ceae.

Hirayama & Tanaka (2011) proposed *Lophiotremataceae* for the genus *Lophiotrema*. The taxonomic concept of the family was later expanded by Hashimoto *et al.* (2017) to accommodate several novel genera with species that are morphologically and phylogenetically distinct from *Lophiotrema*. This included *Atrocalyx*, typified by *A. lignicola* (formerly *Lophiotrema lignicola*), with *A. acutisporus* as a second species. Both species produce small, immersed perithecia bearing large crest-like ostiolar necks and 1-septate ascospores encased by a conspicuous sheath (Hashimoto *et al.* 2017). *Atrocalyx* contains nine species registered in Index Fungorum (November, 2023; indexfungorum.org), all of which, apart from the recently described *A. quercus*, have a known sexual morph (Hyde *et al*. 2020). Pycnidial asexual morphs of *Atrocalyx* (observed in *A. acutisporus*, *A. krabiensis* and *A. quercus*) have globose to subglobose pycnidia with a papillate ostiolar neck (Hashimoto *et al*. 2017, Jayasiri *et al*. 2019, Hyde *et al*. 2020). The ecology and host specificity of *Atrocalyx* spp. are largely unknown although they have been isolated from bark, seed pods and bamboo (Hyde *et al*. 2016, Jayasiri *et al*. 2019, Andreasen *et al*. 2021). Reports are limited to Europe (Andreasen *et al*. 2021) and Asia (Hashimoto *et al*. 2017).

Nigrograna was introduced for a medically important species *N. mackinnonii* (originally described as *Pyrenochaeta mackinnonii*), which causes eumycetomas in humans (De Gruyter *et al*. 2012). The genus *Nigrograna* is comprised of 27 species (as registered in Index Fungorum, November, 2023; indexfungorum.org), isolated from various habitats such as wood, hive-stored pollen, stromatic fungi, human eumycetomas and as endophytes of healthy trees (de Gruyter *et al*. 2012, Jaklitsch & Voglmayr 2016, Kolařík *et al.* 2017, Zhao *et al*. 2018, Boonmee *et al*. 2021). Most *Nigrograna* spp. are difficult to distinguish morphologically, producing superficial perithecia containing brown, 3-septate ascospores that lack a gelatinous sheath. An associated pycnidial morph has been reported from natural substrates for *N. asexualis*, *N. fuscidula*, *N. mycophila*, *N. magnoliae*, *N. samueliana* and *N. rhizophorae*, while *N. mackinnonii* produces pycnidia in culture (De Gruyter *et al*. 2012, Jaklitsch & Voglmayr 2016, Dayarathne *et al*. 2020, Wanasinghe *et al*. 2020, Lu *et al*. 2022). Based on phylogenetic analyses and the description of colony phenotypes, Kolařík *et al*. (2017) described four non-sporulating species as *N. antibiotica*, *N. carollii*, *N.*

peruviensis, and *N. yasuniana* (Kolařík 2018). Some species, such as *N. antibiotica*, produce numerous naphthoquinone derivative metabolites with associated biological activities (Stodůlková *et al.* 2014).

Our two species from the bark of sugar maple are described here as *Atrocalyx glutinosus sp. nov*. and *Nigrograna rubescens sp. nov*. Colony morphologies of axenic cultures on various media were characterized for both species. Micro-morphological characters of the asexual states observed *in vitro* were compared with literature descriptions of other species of their respective genera. Species novelty is supported by multi-locus phylogenetic analyses of rDNA (ITS, including intergenic spacers and partial 28S) and partial protein coding DNA sequences for the second largest subunit of the DNA-directed ribosomal polymerase II gene (*RPB2*) and translation elongation factor 1-alpha gene (*TEF-1α*).

MATERIALS AND METHODS

Fungal growth media

For formulations of the following media, refer to Samson *et al*. (2000): Bacto malt extract agar (MEA), BDH potato dextrose agar (PDA), BDH yeast extract sucrose agar (YES), Commercial dichloran 18 % glycerol agar (DG18), and Sigma cornmeal agar (CMA). Water agar supplemented with autoclaved *A. saccharum* bark was prepared by adding 15 g of Bacto agar to 1 L of water, autoclaved for 20 min, followed by adding to the cooled solidified plates, three pieces of autoclaved (60 min), sterilized bark weighing 1 g.

Specimen collection

Bark samples were selected from fallen *Acer saccharum* collected in Eastern Ontario, Canada in autumn 2019 and spring 2021. Fungal cultures were isolated from bark samples using particle filtration with dilution culturing concepts described in Overy *et al*. (2019). Bark samples were ground using an IKA AII basic grinding mill (Staufen, Germany) for approximately 5 s and subsequently mixed into a slurry with 250 mL of sterile water. The slurry was then vacuum-filtered through a sterile sieve column (Cole-Parmer, Illinois) with decreasing filter pore sizes of 500, 360, 250, and 125 µm. The 125 µm pore size filter was transferred into 50 mL of sterile water in a conical Falcon centrifuge tube, vortexed to release the particles, and following removal of the filter, centrifuged at 3 500 rpm for 3 min to pellet the particles. The supernatant was removed, and the particle pellet was resuspended in 25 mL of sterile water containing 0.5 mL penicillin (10 000 units/mL) and streptomycin (10 mg/mL) (ThermoFischer Scientific, Massachusetts). Each suspension was serially diluted 500× and 3 000× and 40 µL aliquots of the diluted particle suspensions were dispensed into separate wells of a CELLTREAT 48 well tissue culture plate, with each well containing 400 µL of solidified MEA. Plates were incubated in the dark at 25 °C for 8 wk and monitored regularly for fungal growth. When mycelium was observed, it was transferred with tweezers to an isolation plate containing MEA and serially transferred as necessary until axenic cultures were obtained.

Morphological analysis

Four representative axenic strains of each species (based on similarity of colony phenotype), from samples originating either from different sampling sites or obtained either in 2019 or 2021, were cultured on five growth media (MEA, PDA, YES, DG18 and CMA) and observations of colony and micro-morphological characters were made. Culture plates were incubated in darkness at 25 °C and culture diameters and micromorphological structures were measured at 28 d; colony coloration was described following the Methuen Handbook of Colour (Kornerup & Wanscher, 1978). To determine cardinal growth temperatures, ex-type cultures from both species (DAOMC 252609 and DAOMC 252610) were also grown on MEA in increments of 5 °C between 10 °C and 30 °C, and at 37 °C, and also on PDA at 25 °C. Colony photographs were taken using an Olympus Tough TG-5 camera (Olympus, Tokyo) with black velvet as a background.

Three strains of the novel *Atrocalyx* sp. (DAOMC252609, CHEM 2138, CHEM 2208) and four strains of the novel *Nigrograna* sp. (DAOMC252610, CHEM 2166, CHEM 2269, and CHEM 2445) were also grown on WAM for approximatively 6 mo, to induce the formation of reproductive structures. Squash mounts of pycnidia were prepared in lactic acid on microscope slides and heated under a flame for up to 5 s to remove air bubbles. Cultures were examined using an Olympus SZX12 dissecting microscope and BX50 compound microscope (Olympus, Tokyo), and photographed using Infinity 2 or Infinity X USB microscope cameras, using Infinity Capture software (Lumenera, Ottawa). For both species, 50 conidia were measured and up to 10 conidiophore/conidiogenous cells were measured when possible and the mean, standard error and Q values (length/width) were calculated using Excel 2016 (Microsoft, Redmond).

DNA extraction, sequencing, and analyses

To obtain gDNA, mycelia were scraped from the surfaces of 2-wk-old axenic cultures using a sterile scalpel and extracted using the DNeasy UltraClean Microbial Kit (Qiagen, Hilden) following the manufacturer's protocol. Extracted gDNA was quantified using a QUbit Fluorometer 2.0 (Invitrogen, Massachusetts). The internal transcribed spacer (ITS), the Large Ribosomal subunit (LSU; 28S), translation elongation factor-1-alpha (*TEF-1α*) and DNA-directed RNA polymerase II second largest subunit (*RPB2*) were amplified by polymerase chain reaction (PCR) using PuReTaq™ Ready-to-go PCR Beads (Cytiva, Massachusetts). The primers used for PCR amplification were as follows: for the ITS locus, ITS4 and ITS5 (White *et al*. 1990); for the LSU locus, LROR and LR5 (Moncalvo *et al.* 2000); for the partial *RPB2* gene, RPB2-5F and RPB2-7cr (Liu *et al.* 1999); and for the *TEF-1α* gene, EF-526F, EF-983F, EF-1567R and EF-2218R (Rehner *et al.* 2005). All amplification protocols used in this study are provided in Table S1.

To assess the classification and phylogenetic distinctiveness of the new species under study, published reference sequences of the ITS, LSU, *TEF-1α* and *RPB2* loci of previously described and phylogenetically related species were downloaded from GenBank (Table S2). Because the genera *Atrocalyx* and *Nigrograna* are only distantly related, separate sequence alignments for the two datasets were carried out using MUSCLE v. 3.8.425 (Edgar 2004) as implemented in Geneious v. 2022.0.01 (Biomatter, Aukland). For *Atrocalyx*, sequences for all species of *Cryptocoryneaceae* and *Lophiotremataceae* sequenced by Hashimoto *et al.* (2017) and additional species of *Atrocalyx* described since that revision were used with *Anteaglonium rubescens* (CBS 143911) as the

outgroup. For *Nigrograna*, sequences from all species for which sequences of at least three loci used in this study were used, with *Occultibambusa bambusae* (MFLUCC 15-1212) as the outgroup. All alignments were manually trimmed in Geneious v. 2022.0.01 to remove superfluous ends, and for the ITS loci specifically, to remove sites which contained gaps in more than 50 % of the sequences in the alignment. Phylogenetic trees were constructed using both Maximum likelihood (ML) and Bayesian inference (BI) methods. For ML, the IQ-TREE web server (Trifininopoulos *et al.* 2016, accessed 20 October 2023) was used for individual loci using default settings where the model used was automatically determined during the analysis. For the ML concatenated multi-gene analysis, each locus was partitioned and the best model for each partition was determined using ModelFinder and replicated 1 000 times using ultrafast bootstrapping (Trifinopoulos *et al*. 2016, Kalyaanamoorthy *et al*. 2017, Hoang *et al*. 2018). The BI analyses for individual loci were done using MrBayes v. 3.2 (Ronquist *et al.* 2011) with the GTR + G + I model. For the BI concatenated multi-gene analyses, each locus was partitioned and analysed using a mixed model sampling thorough the General Time Reversible (GTR) space. All BI analyses were done using four simultaneous Markov chains until split frequency reached < 0.01, for which convergence was deemed attained. Sample frequency was 1 in 500 generations, with the first 25 % of trees discarded as burn-in. The adequate convergence value was confirmed by ensuring that the average estimated sample size value was higher than 100 and the PSRF+ value was ≈ 1.000 (with values ± 0.05 accepted) for each parameter. Trees were observed and modified using FigTree v. 1.4.3. (Rambaut 2016). All alignments used in the study are deposited on Figshare (https://figshare.com/articles/figure/Nigrograna_rubescens_and_Atrocalyx_glutinosus_alignment_for_individual_datasets/23816805).

Secondary metabolite characterization

For secondary metabolite characterization of *N. rubescens*, three agar plugs were harvested from cultures grown on YES medium at 25 °C, in the dark, after 28 d. Agar plugs were transferred to borosilicate, 20 mL scintillation vials, to which 15 mL of ethyl acetate was added and shaken on an orbital shaker at 200 rpm for 3 h. The supernatant was removed, added to clean vials and the solvent was removed *in vacuo*. The residue was suspended in 1 mL of methanol and transferred to 2 mL vials for metabolite profiling.

Chromatographic analysis of the *N. rubescens* extracts were performed using a Dionex Ultimate 3000 ultra-high performance liquid chromatography (UHPLC) system. Five µL of methanolic metabolite solution was separated using a Phenomenex Kintex C18 column (50 × 2.1 mm, 1.7 µm) that was equilibrated to 30 °C. Mobile phases consisted of A: Water with 0.1 % v/v formic acid and B: Acetonitrile with 0.1 % v/v formic acid. Metabolites were eluted with a 0.35 mL/min flow rate with the following gradient: hold at 5 % B (0–0.5 min), increasing from 5 % to 95 % B (0.5–4.5 min), hold at 95 % B (4.5–8.0 min), decreasing from 95 % to 5 % B (8.0–8.5 min) and re-equilibration at 5 % B (8.5–11.5 min).

All mass spectra were collected using a Thermo Fisher Scientific LTQ Orbitrap XL operated in positive electrospray ionization (ESI+) mode with a voltage of 4.0 kV during 0.5 – 10 min of chromatographic elution. The ESI source was operated with the following settings: sheath gas (40), auxiliary gas (5), sweep gas (2), and capillary temperature (320 °C), tube lens (-100 V). MS^1 spectra were collected with a range of 100–2 000 *m/z* (mass/charge ratio) at 30 k (at *m/z* 400) resolution, automatic gain control target set to 5.0E5, with a max injection time of 500 ms. MS^2 spectra were collected using higher-energy collisional dissociation (HCD) using a collision energy of 30, isolation window of 1.8 *m/z* and a resolution of 15 k. The automatic gain control target was set to 5.0E5 with a max injection time of 1 024 ms. All MS^1 and MS^2 spectra were viewed using Xcalibur's Qual browser (ThermoScientific). MS^2 spectra were averaged with 3–6 spectral averages and converted to spectrum lists then imported into MS-Finder v. 3.52. Queries were created manually with spectrum lists and processed with the default MS-Finder settings.

The clear colourless exudate produced by *A. glutinosus* was harvested from cultures on MEA after 28 d, dissolved in water and analyzed using hydrophilic interaction liquid chromatography (Merck/EMD Millipore, SeQuant ZIC®-cHILIC 100 Å, 2.1 × 100 mm, 3 µm equipped with a 20 × 2.1 mm guard column maintained at 30 °C) on the same UHPLC-HRMS equipment. Mobile phases consisted of C: water with 5 mM ammonium acetate and D: acetonitrile. Metabolites were eluted with a 0.350 mL/min flow rate with the following gradient: hold at 90 % D (0–0.5 min), decreasing to 40 % D (0.5–5.0 min), hold at 40 % D (5.0–7.0 min), increasing to 90 % D (7.0–7.5 min), and re-equilibration at 90 % D (7.5–10.5 min). The mass spectrometer was operated in ESI- mode scanning an *m/z* range of 100–2 000 Da at a resolution of 30 000 in profile mode. The ESI source was operated with the following settings: sheath gas (45), auxiliary gas (10), sweep gas (0), spray voltage (3.2 kV), capillary voltage (-35 V), capillary temperature (320 °C), tube lens (-100 V) and FTMS full scan maximum injection time (500 ms). An aliquot of the clear colourless exudate was also dissolved in deuterated water and a ^{1}H NMR spectrum was acquired with a standard pulse sequence on a Bruker Avance II 500 MHz NMR spectrometer using a 5 mm triple resonance inverse probe with Z-gradient coils.

RESULTS

Phylogenetic analysis & secondary metabolite production of *Atrocalyx*

For our first set of unidentified strains of *Lophiotremataceae*, nBLAST analyses of each DNA sequence alignment (ITS, LSU and *RPB2* loci) suggested that the strains represented a species of *Atrocalyx*. Because of inconsistent taxon sampling in the datasets for the different genes, it was difficult to apply genealogical concordance to support a phylogenetic concept for all species. However, to evaluate phylogenetic structure within the genus, a multigene phylogenetic analysis was conducted using concatenated fragments measuring 507 bp for ITS, 862 bp for LSU and 800 bp for *RPB2*, for a total dataset of 2 169 bp, including gaps (Fig. 1). Most *Atrocalyx* species were statistically poorly supported, except for the phylogenetic relationship between *A. nordicus* and *A. glutinosus* as sister taxa (Fig. 1). The four strains under study represented a putative new species, *A. glutinosus*, differing from other *Atrocalyx* spp. only by 0–2 nucleotides per locus.

Cladograms for phylogenetic analyses of individual loci are provided as supplementary material (Figs S1–3). Phylogenetic analysis of the ITS locus (Fig. S1) suggests that *A. glutinosus* is most closely related to *A. nordicus*, although with poor

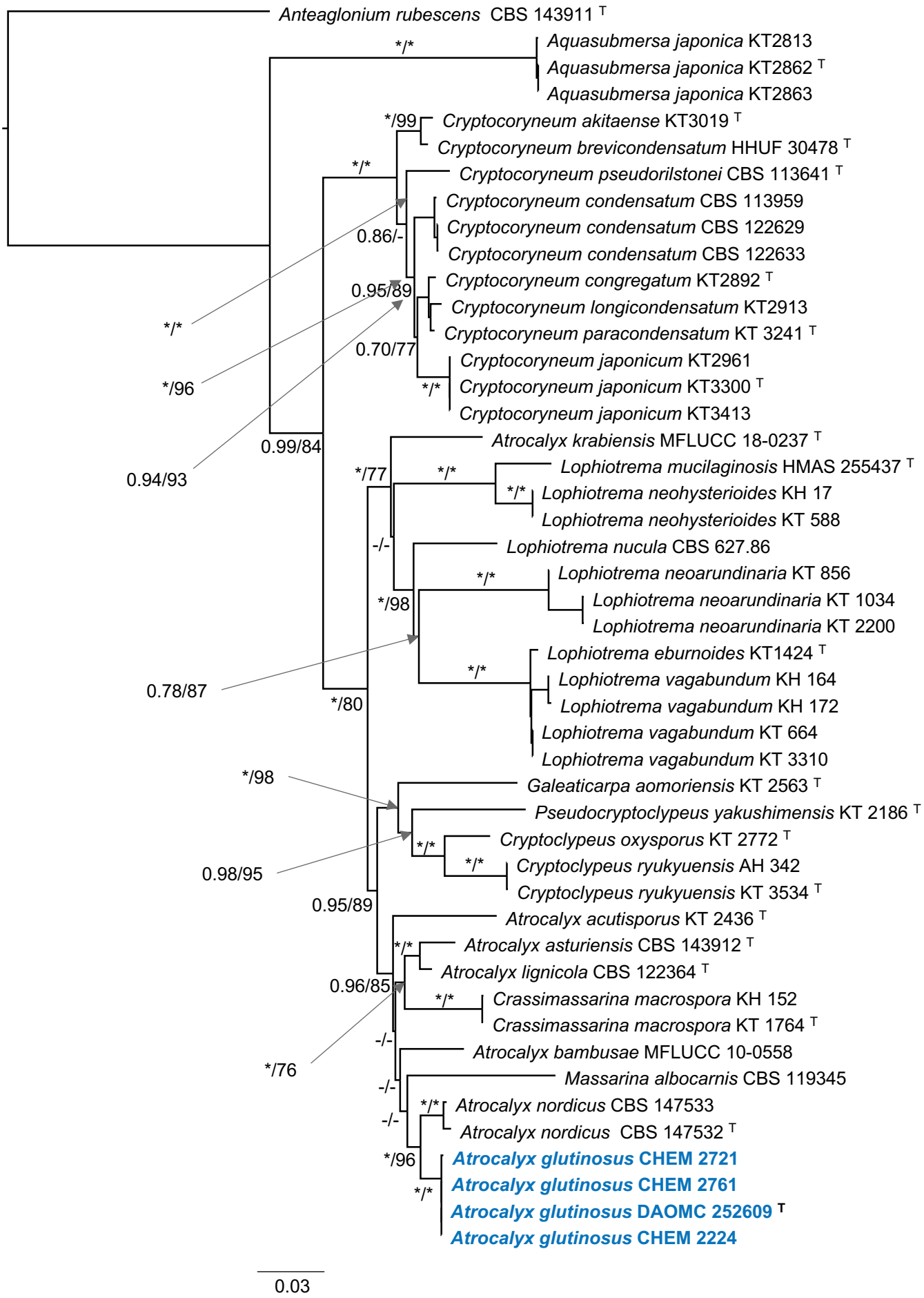

Fig. 1. Phylogenetic tree of the best ML tree obtained using IQ-TREE of a combined ITS, LSU, and *RPB2* dataset of *Lophiotremataceae* and *Cryptocorynaceae*, including *A. glutinosus* in bold and *Anteaglonium rubescens* as an outgroup. Label values are given as BI/ML with values inferior to 0.7/70 replaced with a hyphen (-) and BI/ML values of 1/100 replaced with an asterisk (*), T indicates sequences derived from ex-type specimens or cultures.

statistical support (BI < 70, ML < 90) for most branches. The ITS of *A. glutinosus* is 99.3 % similar to *A. nordicus*, differing by 4 nucleotides and no gaps. The phylogenetic structure revealed by LSU sequences (Fig. S2) was also inconclusive because of poor statistical support for most branches, but *A. glutinosus* was 99.9 % similar to *A. nordicus*, differing by one nucleotide and no gaps. In the *RPB2* analysis (Fig. S3), *A. glutinosus* occurred as a sister group to *A. nordicus* with high statistical support. The *RPB2* sequence of the ex-type of *A. glutinosus* was 94.3 % similar to the ex-type of *A. nordicus*, differing by 41 nucleotides and no gaps. Sequences of *TEF-1α* obtained from *A. glutinosus* were not used for phylogenetic analysis, because comparable sequences of *A. nordicus* are unavailable.

A unique feature distinguishing *A. glutinosus* from other described *Atrocalyx* spp. is the copious production of a sticky, clear exudate when cultured on MEA. UHPLC-HRMS profiles of the exudate suspended in water revealed two chromatographic peaks at a retention time of 5.49 and 5.65 min with an associated pseudomolecular ion in ESI$^-$ mode corresponding to an [M-H]$^-$ of 179.0561 *m/z* that matched our D-glucose chemical standard (Fig. S4). The fungal exudate was dissolved in deuterated water and the ^{1}H NMR spectrum obtained matched that of pullulan (Fig. 2), with some additional peaks corresponding to a free hexose. ^{1}H NMR experiments comparing a pullulan standard and a mixture of pullulan and D-glucose analytical standards confirmed that the *A. glutinosus* exudate was a mixture of pullulan containing additional D-glucose.

Phylogenetic analysis & secondary metabolite production of *Nigrograna*

For the second set of unidentified strains putatively assigned to *Nigrograna*ceae, nBLAST searches suggested that the strains represented a species of *Nigrograna*. As with *Atrocalyx*, we were unable to apply genealogical concordance to support a phylogenetic concept for all species, because of inconsistent taxon sampling for the different genes. Phylogenetic relationships of our strains with related species were evaluated using a multigene analysis of our ITS, LSU, *TEF-1α* and *RPB2* alignments, using sequences derived from specimens or cultures for which at least three loci were available (Fig. 3). Fragments measuring 426 bp for ITS, 778 bp for LSU, 691 bp for *TEF-1α* and 718 bp for *RPB2*, were concatenated into a 2 613 bp long dataset (including gaps). While the phylogenetic placement of most species of *Nigrograna* was well supported, basal clades and several species belonging to the *N. mackinnonii* clade lacked support. The four examined strains of our new species, described as *Nigrograna rubescens* below, differ among each other by 0–2 nucleotides. *Nigrograna aquatica*, *N. locuta-pollinis* and *N. sichuanensis* are sister species to *N. rubescens* with full statistical support (full BI support and 97 ML support).

Cladograms for phylogenetic analyses of individual loci are provided as supplementary material (Figs S5–8). The ITS locus alone provided good overall resolution of *Nigrograna* (Fig. S5): the closest neighbors to *N. rubescens* were *N. aquatica*, *N. locuta-pollinis*, and *N. sichuanensis*, each of which were resolved into distinct species clades. From a nBLAST analysis of the ITS sequence, *N. rubescens* was most similar to *N. sichuanensis*, differing by 6 nucleotides and 1 gap. A comparable level of species resolution was observed for the LSU locus (Fig. S6), where isolates of *N. rubescens* formed a distinct clade separate from other species of *Nigrograna.* The nearest neighbor, *N. locuta-pollinis* differed from *N. rubescens* by 5 nucleotides and no gaps. Phylogenetic analyses of the *TEF-1α* (Fig. S7) clustered *N. rubescens* as sister to *N. locuta-pollinis* and *N. sichuanensis*, but without statistical support on both ML and BI models. Of the species, *N. sichuanensis* was the most similar to *N. rubescens* differing by 12 nucleotides and no gaps. Phylogenetic analysis of the *RPB2* (Fig. S8) placed *N. rubescens* as sister species to *N. locuta-pollinis* though they differed by 43 nucleotides and no gaps. No protein-coding sequences were available for *N. aquatica* and no *RPB2* sequences were available for *N. sichuanensis*.

UPLC-HRMS profiling of *N. rubescens* culture extracts revealed the production of a family of secondary metabolites, based on multiple chromatographic peaks with shared pseudo-molecular ions. A pseudomolecular ion with a *m/z* of 323.1117 was observed to have multiple chromatographic peaks including two peaks at retention times of 3.85 min (major) and 4.27 min

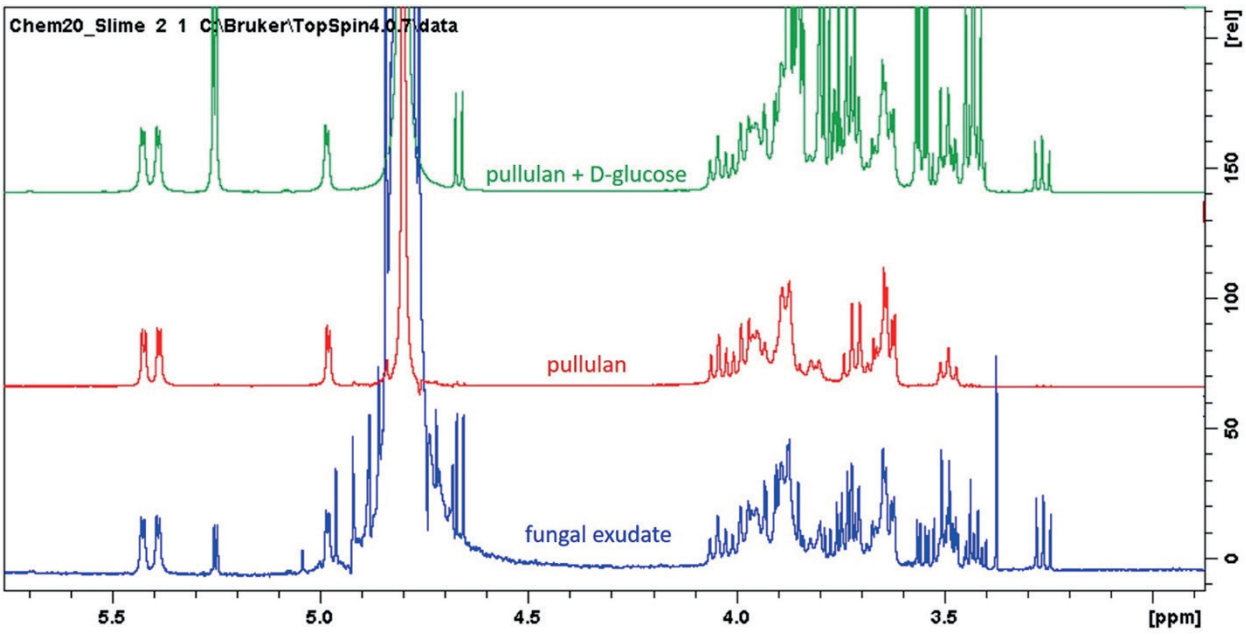

Fig. 2. ^{1}H NMR spectra of a pullulan mixture of D-glucose (top), pullulan (middle) and the fungal exudate (bottom); molecular structure of pullulan is overlaid (middle).

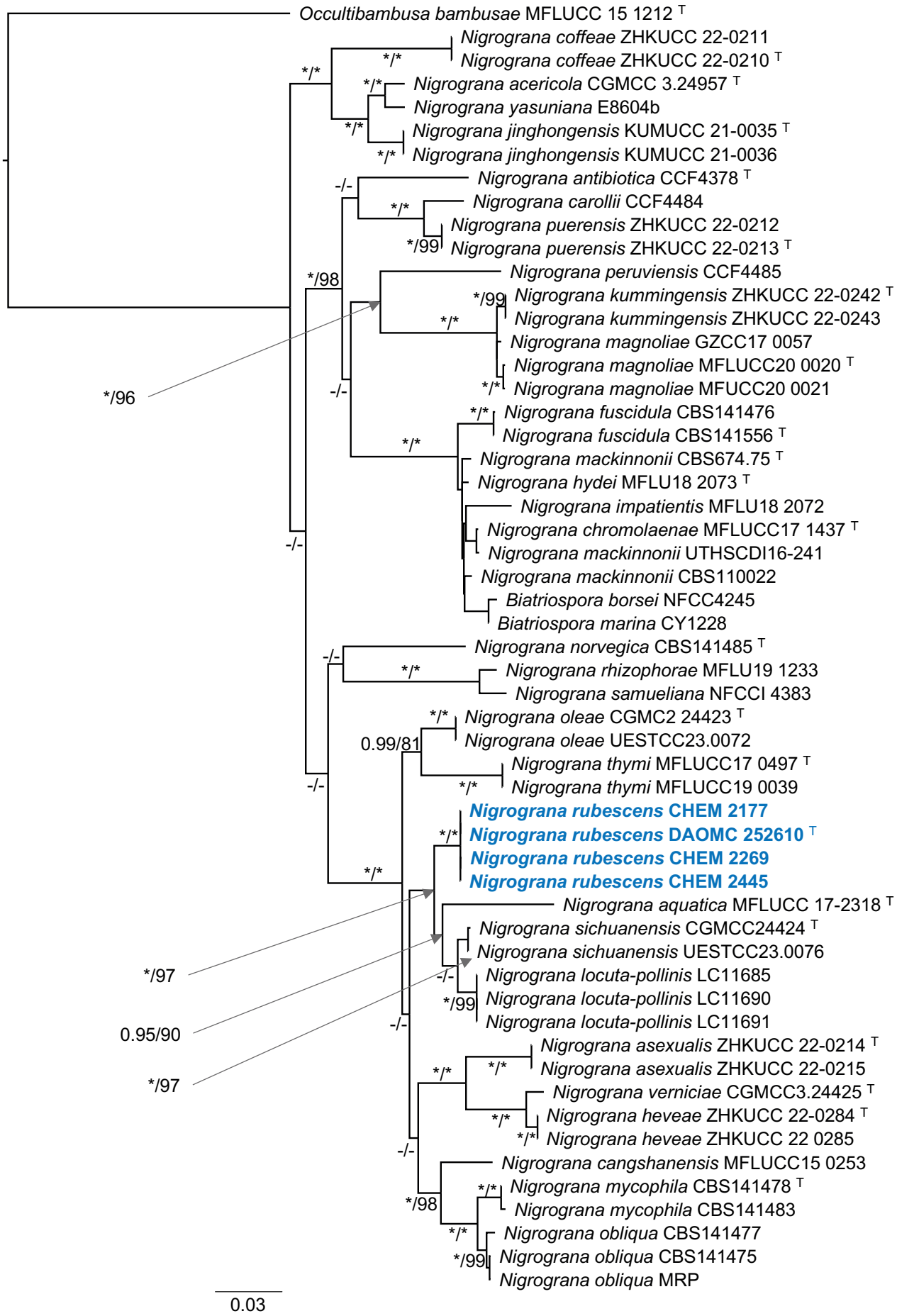

Fig. 3. Phylogenetic tree of the best ML tree obtained using IQ-TREE of a combined ITS, LSU, *TEF-1α*, and *RPB2* dataset with selected species of *Nigrograna*, including *N. rubescens* in bold and *Occultibambusa bambusae* as an outgroup. Label values are given as BI/ML with values inferior to 0.7/70 replaced with a hyphen (-) and BI/ML values of 1/100 replaced with an asterisk (*), [T] indicates sequences derived from ex-type specimens or cultures.

(minor) (Fig. S9). From the MS^1 data (Fig. 4A), *m/z* 323.1117 was consistent with an $[M+H]^+$ adduct as confirmed by a corresponding retention time and chromatographic peak shape of associated pseudomolecular ions representing adducts and neutral loss fragments: $[M+Na]^+$ (*m/z* 345.0937), $[M+H-H_2O]^+$ (*m/z* 305.1011), $[M+H-2H_2O]^+$ (*m/z* 287.0909) and $[M+H-H_2O-CH_3]^+$ (*m/z* 272.0678). While not the major adduct observed, the $[M+H]^+$ precursor mass was chosen for further analysis to provide the greatest chance of obtaining a spectral similarity match when using MS-Finder.

MS-Finder analysis yielded a predicted molecular formula of $C_{16}H_{18}O_7$ (2.9 ppm mass error, 3.78 isotope match score) that had an unsaturation index of 8. Database matching of the resultant MS^2 spectra from *m/z* 323.11 showed moderate similarity to the naphthoquinones dihydroaltersolanol and dihydroaltersolanol C (Fig. 4). While this evidence is not compelling enough to make an absolute identification of the metabolites as dihydroaltersolanols – because of the potential for structural isomers resulting from varied positions of the multiple hydroxyl functional groups appended to the ring system – several metabolites observed by UHPLC-HRMS/MS profiling are naphthoquinones. Eleven different naphthoquinone secondary metabolites were reported from *N. antibiotica*, which include 6-deoxyanhydrofusarubin, 6-deoxyfusarubin, 6-deoxybostrycoidin, balticol A, ascomycones A & B, pleorubrin A-D, and herbarin (Stodůlková *et al.* 2014). However, none of these molecules have a reported $[M+H]^+$ of *m/z* 323.1117. Culture extracts also included additional metabolites with a $[M+H]^+$ of *m/z* 305.1010 and sharing common MS^2 fragmentation patterns that match the $[M+H]^+$ *m/z* of herbarin (as reported from *N. antibiotica*). Commercial standards are unavailable for the naphthoquinones reported from *N. antibiotica*, thus scaled up fermentation, extraction and molecule purification followed up by NMR-based structural elucidation experiments are necessary to fully characterize the naphthoquinone metabolites produced by *N. rubescens*.

Taxonomy

Atrocalyx glutinosus J. Mack & Overy, ***sp. nov.*** MycoBank MB 849672. Fig. 5.

Etymology: From *glutinosa* (Latin), referring to the sticky gel (pullulan) produced by this species in culture on MEA.

Typus: **Canada**, Ontario, Sharbot Lake, Tryon Road woodlot (44°44'6N, 76°41'44W), isolated from milled bark from fallen *Acer saccharum*, 1 Nov. 2019, *J. Mack* (**holotype** DAOM 985072; dried specimen in metabolically inactive state; culture ex-type CHEM 2171 = DAOMC 252609); GenBank ITS = OQ400918; LSU = OQ400928; *TEF-1α* = OQ413076; *RPB2* = OQ413081.

Description: Colonies on MEA at 25 °C, flat to irregularly slightly raised, margin usually entire, slightly felty, producing copious hyaline, sticky droplets of exudate (pullulan); Platinum to Dark Gray, with numerous dark spots where exudate droplets have dried; reverse black. Colonies on PDA at 25 °C, irregularly raised, wavy or occasionally sulcate, margin irregular, velvety to cottony, exudate droplets scarce and inconspicuous, hyaline, sticky; uniformly Light Gray to Medium Gray; reverse black. Colonies on DG18 at 25 °C, strongly raised, irregular, lumpy, crateriform and with irregular margins, velvety, exudate rarely produced as small droplets near the centre of the colonies; Medium Gray, uniformly colored; reverse black. Colonies on YES at 25 °C, strongly crateriform, very irregular and lumpy, radially sulcate on the outer half, and circularly sulcate in the centre, velvety, with raised margins, with a strong yeast-like odor, with hyaline, sticky exudate produced as small droplets and forming a thin layer on surrounding agar; mottled in colours ranging from Platinum to Dark Gray; reverse Medium Gray. Colonies on CMA at 25 °C, mostly flat, immersed, hyaline with cottony Dark Gray centre, exudate absent. On MEA, exudate copious at 20, 25 and 30 °C, but not at 15 and 10 °C. Colony diameters after 28 d, MEA at 10 °C, 7–10 mm; at 15 °C, 12–14 mm; at 20 °C, at 15–20 mm; at 25 °C, at 15–25 mm; at 30 °C, 16–18 mm; at 37 °C, no growth; PDA at 20 °C, 15–24 mm; at 25 °C 19–26 mm; DG18 at 25 °C, 11–13 mm; YES at 25 °C, 21–23 mm; CMA at 25 °C, 20–27 mm.

Hyphae in MEA, pale brown, 2–2.5 µm wide, often with darker irregularly globose intercalary cells, 7–12 × 4–9 µm, sometimes covered by gelatinous exudate, 1–2 µm thick. *Asexual morph* rarely observed, isolated conidiomata produced on DG18 after approximatively 4 mo and on WAM after 4–6 mo of incubation at 20 °C. *Pycnidia* are black, solitary, isolated, immersed in agar, approximately 250 µm wide, ostiole not observed. Average conidiomata measurements were not obtained because of their scarcity. Peridium composed of *textura angularis* or *textura globosa*, cells 4–6.5(–7.5) × 3–5 µm, Q = 1–2 (mean 5.3 ± 0.2 × 3.9 ± 0.1, Q = 1.4 ± 0.1) n = 20. *Conidiophores* arising as short chains of angular cells from the interior cells of the peridium. *Conidiogenesis cells* monoblastic hyaline, globose or ampulliform to slightly elongated cells, 4.5–7.5(–10) × (1.5–)2–3.5 µm, Q 2–5 (mean 6.6 ± 0.5 × 2.6 ± 0.2, Q = 3.3 ± -0.2; n = 10). *Conidia* slimy, pale brown, black in mass, aseptate, cylindrical measuring 3–4 × 1–1.5(–2) µm, Q (1.5–)2–3(–4) (mean 3.5 ± 0.1 × 1.4 ± 0.1µm, Q = 2.44 ± 0.1, n = 50). Sexual state unknown.

Additional strains examined (all isolated from *Acer saccharum* bark): **Canada**, Ontario, Sharbot Lake, Tryon Road woodlot), *Jul*. 2019, *J. Mack* (CHEM 2094); *ibid*., Apr. 2021, *J. Mack* (CHEM 2761); Ottawa, Lalande Conservation Park, Aug. 2019, *J. Mack* (CHEM 2151); McCarthy Forest, Nov. 2019, *J. Mack* (CHEM 2224); Vanier, Ottawa, Nov. 2019, *J. Mack* (CHEM 2721).

Notes: *Atrocalyx glutinosus* was isolated relatively frequently from particles of *A. saccharum* bark, from multiple trees of each surveyed site. Direct examination of bark samples with a dissecting microscope failed to reveal any ascomata. Consequently, the sexual morph of this species is currently unknown, limiting morphological comparisons to other species of *Atrocalyx*. Based on our multigene phylogeny, *A. glutinosus* is closely related to *A. nordicus* with strong support. However, unlike *A. glutinosus*, *A. nordicus* is not known to produce pullulan gel on MEA. Further, *A. glutinosus* grows slower in culture on MEA at 20 °C (15–20 mm) than *A. nordicus* (30–34 mm) (Andreasen *et al*. 2021). *Atrocalyx acervatus* was also isolated from *Acer* but differs from *A. glutinosus* by its faster growth rates (23 *vs.* 10 mm on PDA at 20 °C after 14 d) and the production of diffuse pigments in the agar (de Silva *et al*. 2017). Unfortunately, only the ITS locus could be compared for this latter species (Fig. S1), which was 96.5 % similar, differing from *A. glutinosus* by ten nucleotides and one gap. *Atrocalyx acutisporus*, *A. krabiensis* and *A. quercus* also produce a pycnidial asexual morph similar to *A. glutinosus*, either *in situ* or in culture (Hashimoto *et al*. 2017, Jayasiri *et al*. 2019, Hyde *et al*. 2020); however, the

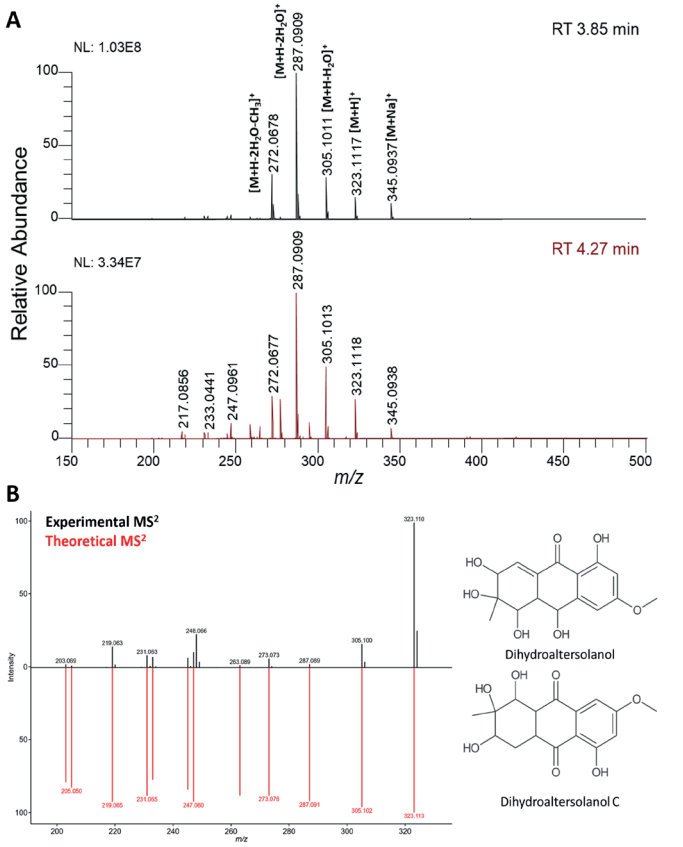

Fig. 4. A. MS[1] spectra for two structurally similar secondary metabolites produced by *N. rubescens* eluting at retention times (RT) of 3.85 and 4.27 min as demonstrated by identical shared protonated, adduct, and neutral loss fragment ions. **B.** MS-Finder spectral matching results of dihydroaltersolanol and dihydroaltersolanol C based on database search using for MS[2] ion fragments from the precursor *m/z* 323.11.

asexual morph of *A. glutinosus* can be distinguished from each of these by its narrower conidia, averaging less than 2 µm wide. Therefore, based on molecular and morphological evidence, we consider *A. glutinosus* a distinct species of *Atrocalyx*.

Nigrograna rubescens J. Mack & Overy, ***sp. nov.*** MycoBank MB 849673. Fig. 6.

Etymology: *Rubescens* (Latin) for reddish or blushing, indicating the dark reddish pigments produced in culture.

Typus: **Canada**, Ontario, Ottawa, McCarthy Forest (45°21'24N, 75°40'29W), isolated from milled bark of a dead *Acer saccharum* tree, 1 Nov. 2019, *J. Mack* (**holotype** DAOM 985073; dried specimen in metabolically inactive state; culture ex-type CHEM 2344 = DAOMC 252610); GenBank ITS = OQ400924; LSU = OQ400934; *TEF-1α* = OQ413077; *RPB2* = OQ413082.

Description: Colonies on MEA at 25 °C, flat, often with a small umbo (2–3 mm diam) at the centre, sulcations radiating from the umbo to near the colony margin, often with abundant aerial hyphae near the centre, coloration variable, Brownish Gray to Grayish Brown, or Olive Gray, colony margin irregularly raised and wavy, felty or cottony; reverse black; soluble pigments relatively opaque, filling plate, Brownish Orange to Dark Brown, Greyish Yellow or Brownish Orange at 20 °C, faint or absent at 10 °C and 15 °C. Colonies on PDA at 25 °C, slightly raised, often with an umbo up to 5–7 mm diam. In the centre, sulcations radiating from the umbo to nearly the colony margin, margin irregular; cottony or felty, Platinum Gray to Medium Gray; reverse black; soluble pigments relatively opaque, filling plate, Brown to Dark Brown, or Grayish Yellow to Olive at 20 °C. Colonies on DG18, rather flat, radially sulcate, somewhat irregular, smooth or faintly velvety, margin Pastel Gray and centre of colonies Dust Gray; reverse black; soluble pigments black and opaque, diffusing up to 10 mm from colonies. Colonies on YES highly raised and strongly sulcate; smooth or slightly crinkled, Brownish Gray; reverse black; volatile odor pleasant, reminiscent of decaying litter or chocolate; soluble pigments black, opaque. Colonies on CMA irregular, mostly immersed, except for a few scattered hyphae in the centre, hyaline and lacking diffuse pigments. Colony diameters after 28 d: on MEA at 10 °C, 9–10 mm; at 15 °C, 16–18 mm; at 20 °C, 17–22 mm; at 25 °C, 15–20 mm; at 30 °C, 12–14 mm; at 37 °C, no growth; on PDA, at 20 °C, 30–45 mm; at 25 °C, 28–38 mm; on DG18 at 25 °C, 22–24 mm; on YES at 25 °C, 52 –56 mm; on CMA at 25 °C, 35–40 mm.

Hyphae pale brown, 1–1.5 µm wide, swollen, dark cells either intercalary or apical on aerial hyphae in DG18 after approximatively four months of incubation, 12–20(–22) × 10–18(–20) µm. *Asexual morph* rarely observed but produced on WAM after several months of incubation at 20 °C, or more rarely on MEA after 1 mo. On MEA, *conidiomata* deeply embedded in the mycelium, and not visible unless aerial hyphae are vigorously scraped; on WAM, conidiomata are pycnidial, black, solitary, or gregarious, up to 600 µm wide, mostly immersed in agar or sterilized *A. saccharum* bark; ostiolar neck measuring up to 250 × 50 µm, ostiole and exuding conidial mass not observed. *Peridium* up to 35 µm wide, outer layers black, progressively becoming hyaline in the inner layers, composed of *textura angularis*, cells 5–8 × 2–4.5 µm (mean: 6.4 ± 0.2 × 2.8 ± 0.2 Q = 2.5 ± 0.2). *Conidiophores* arising from interior of conidiomatal wall, sparsely branched, multi-septate, up to 30 µm long, and 2 µm wide. *Conidiogenous cells* phialidic, acropleurogenous, intercalary or terminal, variable in length, up to 7 µm long and 1 µm wide. *Conidia* smooth, hyaline, aseptate, cylindrical, 2.5–3.0(–3.5) × 0.5–1.5 µm, Q = 2–4(–4.5) (mean: 2.9 ± 0.3 × 1 ±0.2 µm, Q = 3.1 ± 0.1, n = 50). *Sexual state* unknown.

Additional strains examined (all isolated from bark of *Acer saccharum*): **Canada**, Ontario, Sharbot Lake, Tryon Road woodlot, Oct. 2019, *J. Mack* (CHEM 2177); Vanier, Ottawa, Nov. 2019, *J. Mack* (CHEM 2266); *ibid*., (CHEM 2445).

Notes: *Nigrograna rubescens* occurs on the bark of *A. saccharum* and was often isolated using particle filtration and dilution culturing; however, no associated sexual state was observed on the original samples. Based on our multilocus phylogeny, *N. rubescens* is most closely related to *N. locuta-pollinis*, *N. sichuanensis* and *N. aquatica*. *Nigrograna locuta-pollinis* can easily be distinguished from *N. rubescens* by its much faster growth rate, reaching 49 mm on PDA at 25 °C after 2 wk (Zhao *et al.* 2018). *Nigrograna sichuanensis* produces yellow diffusing pigments on PDA unlike *N. rubescens* which produce dark opaque diffuse pigments (Li *et al*. 2023) and *N. aquatica* grows slower, reaching 25 mm on PDA at 25 °C after 30 d (Dong *et al*. 2020) with colonies lacking the diffusing pigments characteristic of *N. rubescens*. Unfortunately, no coelomycetous asexual morph is known for any of these species in culture, making further comparison difficult. However, six species of *Nigrograna* (*N. asexualis*, *N. fuscidula*, *N. mycophila*, *N. norvegica*, *N.*

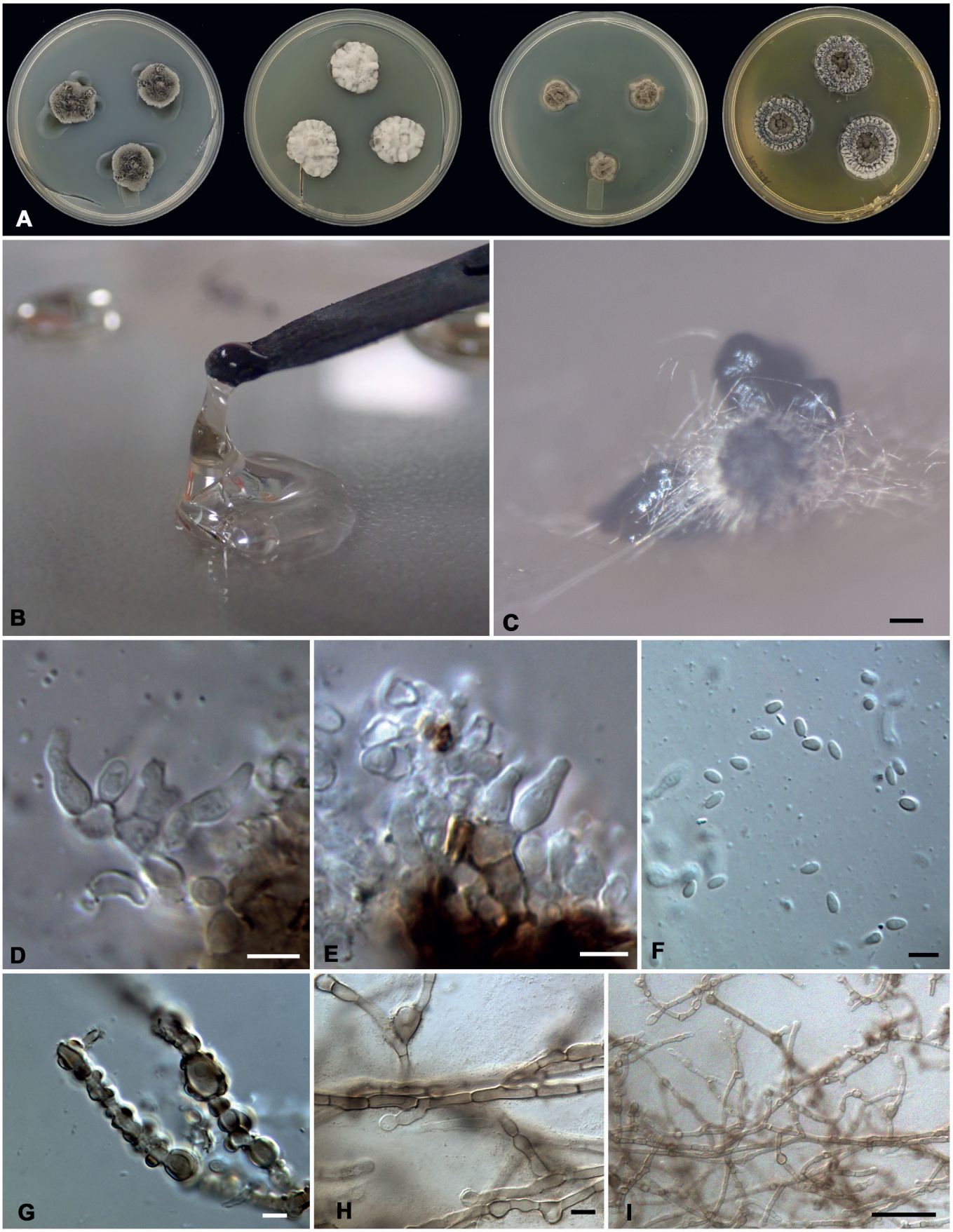

Fig. 5. *Atrocalyx glutinosus.* **A.** Colony morphology (28 d) from left to right: MEA, PDA, DG18, YES. **B.** Pullulan gel. **C.** Colonies in culture on WAM. **D, E.** Conidiogenous cells. **F.** Conidia. **G–I.** Hyphae. Scale bars: C = 100 µm; D–H = 5 µm; I = 20 µm.

rhizophorae and *N. samueliana*) produce conidiomata *in situ* that are very similar to those of *N. rubescens*; however, *N. rubescens* produce slightly narrower conidia, on average about 1 µm wide (Jaklitsch &Voglmayr 2016, Dayarathne *et al*. 2020, Lu *et al*. 2022). Other species that also produce red pigments in culture, such as *N. antibiotica* and *N. carollii*, might be difficult to distinguish from *N. rubescens* but all species had distinct gene sequences for all examined loci. No asexual morph was reported in cultures of *N. antibiotica* and *N. carollii* (Kolařík *et al*. 2017, Kolařík 2018). Therefore, we consider *N. rubescens* a novel species of *Nigrograna* based on molecular and morphological evidence.

DISCUSSION

In this study, two new species of *Pleosporales* were commonly isolated from ground bark of *Acer saccharum* using particle filtration in combination with dilution culturing. Both species had distinctive morphologies, allowing their identities to be recognized based on culture characters alone, namely the copious production of pullulan by *A. glutinosus* and the soluble dark red pigments of *N. rubescens*. The significance of diagnostic micromorphological characters was hampered by the fact that most species descriptions of *Atrocalyx* and *Nigrograna* species were described solely on their sexual states as observed in nature, and the isolates obtained failed to produce a sporulating asexual state in culture. For both of our new species, prolonged incubation in the dark on a medium containing a maple bark substrate (WAM) elicited the production of some conidiomata, suggesting that a comparable approach could be used to induce sporulation of other species of these two genera in culture.

To induce sporulation of tree bark-derived fungi, media with a higher osmotic potential, such as DG18, might be helpful. DG18 is a low water content medium used to isolate, measure and compare growth rates of xerophilic species (Visagie *et al.* 2014, Black 2020). Because bark has a low water activity, fungi isolated from this substrate and grown on a xerophilic medium might develop structures more typical as those that might occur in nature. For instance, on DG18 *A. glutinosus* produced conidiomata after several months of incubation and *N. rubescens* produced unidentified cells on aerial hyphae that were not observed on other media (Fig. 6E). Another point of interest is that cultures of *N. rubescens* formed only a few pycnidia on MEA after 28 d that were concealed by a thick layer of superficial, vegetative hyphae, that had to be removed before they could be observed. Therefore, careful dissection of colonies may be necessary to observe conidiomata in strains of other species of this genus.

Atrocalyx glutinosus shares a similar corticolous habitat with *A. nordicus*, the most closely related species in our phylogenetic analyses. Some environmental sequences on GenBank are probably conspecific with *A. glutinosus* as they differ by one or two nucleotides on the sequence of their ITS locus. These were detected or isolated from various substrates such as dead wood of *Fagus sylvatica* in Germany (Floren *et al*. 2015; GenBank LC015677), wood of *Vitis vinifera* in Switzerland (Hofstetter *et al*. 2012; GenBank JQ070520), *Hylesinus varius* on *Fraxinus excelsior* in Czech Republic (Kolařík, unpublished; GenBank LR961708, LR961709) and as endophytes in healthy leaves of *Quercus gambelii* in Arizona (U'ren *et al*. 2010; GenBank HM123518). Therefore, *A. glutinosus* might have a broader host and geographic range encompassing both North America and Europe. Interestingly, *A. glutinosus* is the first species of *Atrocalyx* reported in North America. Similarly, several DNA sequences identified as *Lophiostoma cynaroidis* appear to be closely related to *A. glutinosus*. The ITS sequence of the ex-type specimen of *L. cynaroidis* was 98.2 % similar to *A. glutinosus*, differing by 6 nucleotides and 4 gaps. Although Marincowitz *et al*. described *L. cynaroidis* in 2008, Hashimoto *et al.* (2017) did not mention it in their review of the *Lophiotremataceae*. In addition, *L. cynaroidis* lacks sequences for protein coding genes and was only described based on its sexual morph. More study of additional strains and protein coding sequences are necessary to refine the classification of *L. cynaroidis*, but it seems likely to be a species of *Atrocalyx.*

All strains of *A. glutinosus* produced copious amounts of hyaline, transparent, stretchy gel, especially when grown on MEA between 20 and 30 °C. This gel consistently interfered with DNA extractions, and cultures of *A. glutinosus* used for DNA sequencing had to be grown on media such as PDA before DNA could be extracted. Using NMR spectroscopy, the gel was determined to be mostly pullulan and monomeric D-glucose units of the polysaccharide. Pullulan is an edible, but poorly digestible polysaccharide originally isolated from *Aureobasidium pullulans*. It is currently used in the food industry to produce edible films, amongst several other products. Despite its multiple applications, pullulan is rarely used because of associated high production costs (Oğuzhan & Yangılar 2013). Therefore, because *A. glutinosus* produces abundant pullulan, this species might be useful for production of industrial quantities. Interestingly, no other known species of *Atrocalyx* are reported to produce gel exudates, even when grown on MEA, suggesting that this metabolite might be particular to *A. glutinosus*.

We isolated *N. rubescens* from multiple trees at different sites, and this species should be considered a common inhabitant of bark of *A. saccharum*, at least in Eastern Ontario, Canada. The ITS sequences of *N. rubescens* do not match any environmental sequences available in GenBank, suggesting that *N. rubescens* might have a narrow host distribution. Additional sampling of other native trees using particle filtration in the known range of *N. rubescens* would clarify whether this ecological tendency is reliable. Furthermore, additional effort is needed to locate and characterize a putative sexual morph of *N. rubescens* to allow further comparison with other known species of *Nigrograna*. *Nigrograna rubescens* is the second species of *Nigrograna* reported from North America and additional sampling of tree bark could yield more novel species of *Nigrograna*. In this study, *N. rubescens* was found to be the sister species of *N. locuta-pollinis*, *N. sichuanensis* and *N. aquatica*. Unfortunately, the type of *N. aquatica* (MFLU 17-1661) lacks protein coding sequences (Dong *et al.* 2020) which prevented a more thorough phylogenetic comparison with *N. rubescens*. *Nigrograna antibiotica* was also reported to produce diffuse pigments of similar coloration to *N. rubescens*. Our preliminary UHPLC-HRMS/MS analyses of *N. rubescens* extracts confirm the production of naphthoquinone secondary metabolites, having structural similarities to those previously reported from *N. antibiotica* (Stodůlková *et al.* 2014) in extracts of *N. rubescens*. Naphthoquinone secondary metabolites are associated with a broad range of biological activities (Naysmith *et al*., 2017) and those of *N. antibiotica* are antagonistic against the fungus *Pyronema domesticum* and cytotoxic to human adenocarcinoma and fibroblast cell lines (Stodůlková *et al.* 2014).

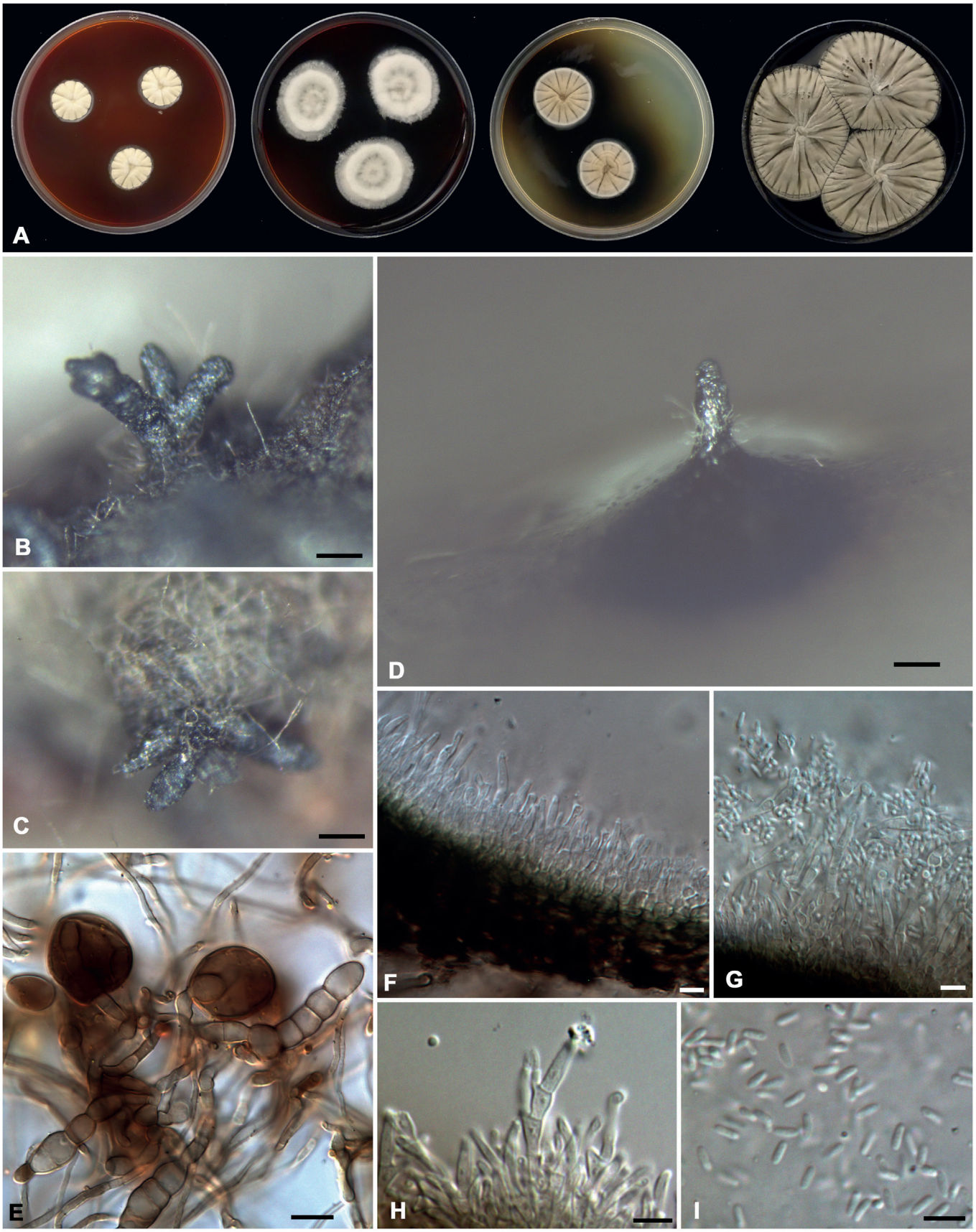

Fig. 6. *Nigrograna rubescens.* **A**. Colony morphology (28 d) from left to right: MEA, PDA, DG18, YES. **B, C**. Ostiolar neck on WAM. **D**. Pycnidium in WAM. **E**. Hyphae and swollen cells on DG18. **F–H**. Conidiophore. I. Conidia. Scale bars: B–D = 100 µm; E = 10 µm; F–I = 5 µm.

ACKNOWLEDGMENTS

We acknowledge the support of A. Hermans in assisting during particle filtration and R. Assabgui for is assistance in the molecular laboratory. We would also like to thank the MTL service at the Ottawa Research and Development Centre (AAFC) for providing reagents and sequencing and T. Rintoul and the DAOM culture collection team for accessioning the cultures. We also thank M. Réblová for her help in reviewing the taxonomy presented in the manuscript and M. Andreasen for providing *RPB2* sequences of *Atrocalyx nordicus* prior to their release on GenBank.

Conflict of interest: The authors declare that there is no conflict of interest.

REFERENCES

Ahmed S, Gerrits van den Ende BHG, Fahal AH, *et al.* (2014). Rapid identification of black grain eumycetoma causative agents using rolling circle amplification. *PLoS Neglected Tropical Diseases* **8**: e3368.

Andreasen M, Skrede I, Jaklitsch WM, *et al.* (2021). Multi-locus phylogenetic analysis of lophiostomatoid fungi motivates a broad concept of *Lophiostoma* and reveals nine new species. *Persoonia* **46**: 240–271.

Ariyawansa HA, Hyde KD, Jayasiri SC, *et al.* (2015). Fungal diversity notes 111–252: taxonomic and phylogenetic contributions to fungal taxa. *Fungal Diversity* **75**: 27–274.

Black WD (2020). A comparison of several media types and basic techniques used to assess outdoor airborne fungi in Melbourne, Australia. *PLoS ONE* **15**: e0238901.

Boonmee S, Wanasinghe DN, Calabon MS, *et al*. (2021). Fungal diversity notes 1387–1511: taxonomic and phylogenetic contributions on genera and species of fungal taxa. *Fungal Diversity* **111**: 1–335.

Dai DQ, Phookamsak R, Wijayawardene NN, *et al.* (2017). Bambusicolous fungi. *Fungal Diversity* **82**: 1–105.

Dayarathne MC, Jones EBG, Maharachchikumbura SSN, *et al*. (2020). Morpho-molecular characterization of microfungi associated with marine based habitats. *Mycosphere* **11**: 1–188.

De Gruyter J, Woundenberg JHC, Aveskamp MM, *et al*. (2012). Redisposition of phoma-like anamorphs in *Pleosporales*. *Studies in Mycology* **75**: 1–36.

De Silva NI, Thambugala KS, Jeewon R, *et al*. (2017). Morphology and phylogeny of *Atrocalyx acervatus sp. nov*. (*Lophiotremataceae*) from *Acer* species. *Phytotaxa* **333**: 199–208.

Dong W, Wang B, Hyde KD, *et al*. (2020). Freshwater *Dothideomycetes*. *Fungal Diversity* **105**: 319–575.

Edgar RC (2004). MUSCLE: a multiple sequence alignment method with reduced time and space complexity. *BMC Bioinformatics* **5**: 113.

Floren A, Krüger D, Müller T, *et al.* (2015). Diversity and interactions of wood-inhabiting fungi and beetles after deadwood enrichment. *PLoS ONE* **10**: e0143566.

Hashimoto A, Matsumura M, Hirayama K, *et al.* (2016). Taxonomy and phylogeny of *Cryptocoryneum* (*Pleosporales*, *Dothideomycetes*). *Mycological Progress* **15**: 45.

Hashimoto A, Matsumura M, Hirayama K, *et al.* (2017). Revision of *Lophiotremataceae* (*Pleosporales*, *Dothideomycetes*): *Aquasubmersaceae*, *Cryptocoryneaceae*, and *Hermatomycetaceae fam. nov*. *Persoonia* **39**: 51–73.

Hoang DT, Chernomor O, von Haeseler A, *et al.* (2018). UFBoot2: Improving the ultrafast bootstrap approximation. *Molecular Biology and Evolution* **35**: 518–522.

Hofstetter V, Buyck B, Croll D, *et al*. (2012). What if esca disease of grapevine were not a fungal disease? *Fungal Diversity* **54**: 51–67.

Hirayama K, Tanaka K (2011). Taxonomic revision of *Lophiostoma* and *Lophiotrema* based on reevaluation of morphological characters and molecular analyses. *Mycoscience* **52**: 401–412.

Hongsanan S, Hyde KD, Phookamsak, *et al.* (2020). Refined families of *Dothideomycetes*: *Dothideomycetidae* and *Pleosporomycetidae*. *Mycosphere* **11**: 1553–2107.

Hyde KD, Hongsanan S, Jeewon R, *et al*. (2016). Fungal diversity notes 367–490: taxonomic and phylogenetic contributions to fungal taxa. *Fungal Diversity* **80**: 1–270.

Hyde KD, Jeewon R, Chen Y, *et al*. (2020). The numbers of fungi: is the descriptive curve flattening? *Fungal Diversity* **103**: 219–271.

Hyde KD, Norphanphoun C, Ma J, *et al.* (2023). Mycosphere notes 387–412 – novel species of fungal taxa from around the world. *Mycosphere* **14**: 663–744.

Jaklitsch WM, Voglmayr HM (2016). Hidden diversity in *Thyridaria* and a new circumscription of the *Thyridariaceae*. *Studies in Mycology* **85**: 35–64.

Jaklitsch WM, Fournier J, Voglmayr H (2018). Two unusual new species of *Pleosporales*: *Anteaglonium rubescens* and *Atrocalyx asturiensis*. *Sydowia* **70**: 129–140.

Jayasiri SC, Hyde KD, Jones EBG, *et al*. (2019). Diversity, morphology, and molecular phylogeny of *Dothideomycetes* on decaying wild seed pods and fruits. *Mycosphere* **10**: 1–186.

Kalyaanamoorthy S, Minh BQ, Wong TFK, *et al.* (2017). ModelFinder: Fast model selection for accurate phylogenetic estimates. *Nature Methods* **14**: 587–589.

Kolařík M, Spacowikz DJ, Gazis M, *et al.* (2017). *Biatriospora* (*Ascomycota: Pleosporales*) is an ecologically diverse genus including facultative marine fungi and endophytes with biotechnological potential. *Plant Systematics and Evolution* **303**: 35–50.

Kolařík M (2018). New taxonomic combinations in endophytic representatives of the genus *Nigrograna*. *Czech Mycology* **70**: 123–126.

Kornerup A, Wanscher JH (1978). *Methuen Handbook of Colour.* 3rd ed. Eyre Methuen, London.

Li WL, Liang RR, Dissanayake AJ, *et al.* (2023). Mycosphere Notes 413–448: *Dothideomycetes* associated with woody oil plants in China. *Mycosphere* **14**: 1436–1529.

Liu JK, Hyde KD, Jones EBG, *et al*. (2015). Fungal diversity notes 1–110: taxonomic and phylogenetic contributions to fungal species. *Fungal Diversity* **72**: 1–197.

Liu YJ, Whelen S, Hall BD (1999). Phylogenetic relationships among ascomycetes: evidence from an RNA polymerse II subunit. *Molecular Biology and Evolution* **16**: 1799–1808.

Lu L, Karunarathna SC, Dai DQ, *et al.* (2022). Three new species of *Nigrograna* (*Dothideomycetes*, *Pleosporales*) associated with Arabica coffee from Yunnan Province, China. *Mycokeys* **94**: 51–71.

Mapook A, Hyde KD, McKenzie EHC, *et al.* (2020). Taxonomic and phylogenetic contributions to fungi associated with the invasive weed *Chromolaena odorata* (Siam weed). *Fungal Diversity* **101**: 1–175.

Marincowitz S, Crous PW, Groenewald JZ, *et al.* (2008). *Microfungi occurring on Proteaceae in the Fynbos*. CBS Biodiversity series 7. Centraalbureau voor Schimmelcultures, Utrecht, The Netherlands.

Moncalvo JM, Lutzoni FM, Rehner SA, *et al.* (2000). Phylogenetic relationships of agaric fungi based on nuclear large subunit ribosomal DNA sequences. *Systematic Biology* **49**: 278–305.

Naysmith BJ, Hume PA, Sperry J, *et al*. (2017). Pyranonapthoquinones – isolation, biology and synthesis: an update. *Natural Products Reports* **34**: 25–61.

Oğuzhan P, Yangılar F (2013). Pullulan: Production and usage in food industry. *African Journal of Food Science and Technology* **4**: 57–63.

Overy PD, Rämä T, Oosterhuis R, *et al*. (2019). The neglected marine fungi, *sensu stricto*, and their isolation for natural products' discovery. *Marine Drugs* **17**: 42.

Phookamsak R, Hyde KD, Jeewon R, *et al*. (2019). Fungal diversity notes 929–1035: taxonomic and phylogenetic contributions on genera and species of fungi. *Fungal Diversity* **95**: 1–273.

Rambaut A (2016). FigTree v. 1.4.0. http://tree.bio.ed.ac.uk/software/figtree/.

Raper KB, Thom C (1949). *Manual of the Penicillia*. The Williams & Wilkins Company, Baltimore, United States.

Rehner A, Buckley E (2005). A *Beauveria* phylogeny inferred from nuclear ITS and EF1-α sequences: evidence for cryptic diversification and links to *Cordyceps* teleomorphs. *Mycologia* **97**: 84–98.

Ronquist, F, Huelsenbeck JP (2003). MRBAYES 3: Bayesian phylogenetic inference under mixed models. *Bioinformatics* **19**: 1572–1574.

Ronquist J, Huelsenbeck J, Teslenko M (2011). MrBayes version 3.2 Manual: Tutorials and Model Summaries. http://mrbayes.sourceforge.net/mb3.2_manual.pdf

Samson RA, Hoekstra ES, Frisvad JC, *et al*. (2000). *Introduction to food- and airborne fungi* 6th edition. Centraalbureau voor Schimmelcultures, Utrecht, The Netherlands.

Schoch CL, Crous PW, Groenewald JZ, *et al.* (2009). A class-wide phylogenetic assessment of *Dothideomycetes*. *Studies in Mycology* **64**: 1–15.

Stodůlková E, Man P, Kuzma M, *et al*. (2014). A highly diverse spectrum of naphthoquinone derivatives produced by the endophytic fungus *Biatriospora* sp. CCF 4378. *Folia Microbiologia* **60**: 259–267.

Suetrong S, Schoch, CL, Spatafora JW, *et al.* (2009). Molecular systematics of the marine *Dothideomycetes. Studies in Mycology* **64**: 155–173.

Sun X, Xu M, Kong W, *et al.* (2022). Fine identification and classification of a novel beneficial *Talaromyces* fungal species from Masson pine rhizosphere soil. *Journal of Fungi* **8**: 155.

Tanaka K, Hirayama K, Yonezawa H, *et al*. (2009). Molecular taxonomy of bambusicolous fungi: *Tetraplosphaeriaceae*, a new pleosporalean family with *Tetraploa*-like anamorphs, and notes on the phylogeny of selected species from bamboos. *Studies in Mycology* **64**: 175–209.

Tanney JB, Seifert KA (2018). *Phacidiaceae* endophytes of *Picea rubens* in Eastern Canada. *Botany* **96**: 555–588.

Tibpromma S, Hyde, KD, Jeewon R, *et al*. (2017). Fungal diversity notes 491–602: taxonomic and phylogenetic contributions to fungal taxa. *Fungal Diversity* **83**: 1–261.

Trifinopoulos J, Nguyen L, von Haeseler A, *et al*. (2016). W-IQ-TREE: a fast online phylogenetic tool for maximum likelihood analysis. *Nucleic Acids Research* **44**(W1): W232–W235.

U'ren JM, Lutzoni F, Miadlikowska J, *et al.* (2010). Community analysis reveals close affinities between endophytic and endolichenic fungi in mosses and lichens. *Plant Microbe Interactions* **60**: 340–353.

Valenzuela-Lopez N, Sutton DA, Cano-Lira JF, *et al.* (2017). Coelomycetous fungi in the clinical setting: morphological convergence and cryptic diversity. *Journal of Clinical Microbiology* **55**: 552–567.

Visagie CM, Houbraken J, Frisvad JC, *et al*. (2014). Identification and nomenclature of the genus *Penicillium*. *Studies in Mycology* **78**: 343–371.

Wanasinghe, DN, Wijayawardene NN, Xu J, *et al*. (2020). Taxonomic novelties in *Magnolia*-associated pleosporalean fungi in the Kunming Botanical Gardens (Yunnan, China). *PLoS ONE* **15**: e0235855.

White TJ, Bruns T, Lee S, *et al*. (1990). Amplification and direct sequencing of fungal ribosomal RNA genes for phylogenetics. In: *PCR protocols: a guide to methods and applications* (Innis MA, Gelfand DH, Sninsky JJ, *et al.*, eds). Academic Press, San Diego (California), USA: 315–322.

Wijayawardene NN, Hyde KD, Dai DQ, *et al.* (2022). Outline of *Fungi* and fungus-like taxa – 2021. *Mycosphere* **13**: 53–453.

Zhang Y, Crous PW, Schoch C, *et al.* (2011). *Pleosporales*. *Fungal Diversity* **53**: 1–221.

Zhang J, Liu J, Thambugala KM, *et al*. (2020). Two new species and a new record of *Nigrograna* (*Nigrograna*ceae, *Pleosporales*) from China and Thailand. *Mycological Progress* **19**: 1365–1375.

Zhao YZ, Zang ZF, Cai L, *et al.* (2018). Four new filamentous fungal species from newly-collected and hive stored bee pollen. *Mycosphere* **9**: 1089–1116.

Supplementary Material: http://fuse-journal.org/

Fig. S1. Phylogenetic tree of the best ML tree obtained using IQ-TREE of the ITS locus dataset of *Lophiotremataceae* and *Cryptocorynaceae*, including *A glutinosus* in bold and *Anteaglonium rubescens* as an outgroup. Label values are given as BI/ML with values inferior to 0.7/70 replaced with a hyphen (-) and BI/MLvalues of 1/100 replaced with an asterisk (*), ^{T} indicates sequences derived from ex-type specimens or cultures.

Fig. S2. Phylogenetic tree of the best ML tree obtained using IQ-TREE of the LSU locus dataset of *Lophiotremataceae* and *Cryptocorynaceae*, including *A glutinosus* in bold and *Anteaglonium rubescens* as an outgroup. Label values are given as BI/ML with values inferior to 0.7/70 replaced with a hyphen (-) and BI/MLvalues of 1/100 replaced with an asterisk (*), ^{T} indicates sequences derived from ex-type specimens or cultures.

Fig. S3. Phylogenetic tree of the best ML tree obtained using IQ-TREE of the *RPB2* gene dataset of *Lophiotremataceae* and *Cryptocorynaceae*, including *A glutinosus* in bold and *Anteaglonium rubescens* as an outgroup. Label values are given as BI/ML with values inferior to 0.7/70 replaced with a hyphen (-) and BI/MLvalues of 1/100 replaced with an asterisk (*), ^{T} indicates sequences derived from ex-type specimens or cultures.

Fig. S4. HILIC chromatogram of the fungal exudate total ion current (top trace); extracted ion chromatogram (XIC) of a hexose sugar $[M-H]^-$ of *m/z* 179.0561 from the fungal exudate data (middle trace); and XIC of a hexose sugar $[M-H]^-$ of *m/z* 179.0561 from profiling of a D-glucose standard using the same HILIC conditions (bottom trace).

Fig. S5. Phylogenetic tree of the best ML tree obtained using IQ-TREE of the ITS locus dataset with selected species of *Nigrograna*, including *N. rubescens* in bold and *Occultibambusa bambusae* as an outgroup. Label values are given as BI/ML with values inferior to 0.7/70 replaced with a hyphen (-) and BI/ML values of 1/100 replaced with an asterisk (*), ^{T} indicates sequences derived from ex-type specimens or cultures.

Fig. S6. Phylogenetic tree of the best ML tree obtained using IQ-TREE of the LSU locus dataset with selected species of *Nigrograna*, including *N. rubescens* in bold and *Occultibambusa bambusae* as an outgroup. Label values are given as BI/ML with values inferior to 0.7/70 replaced with a hyphen (-) and BI/ML values of 1/100 replaced with an asterisk

(*), [T] indicates sequences derived from ex-type specimens or cultures.

Fig. S7. Phylogenetic tree of the best ML tree obtained using IQ-TREE of the *TEF-1α* gene dataset with selected species of *Nigrograna*, including *N. rubescens* in bold and *Occultibambusa bambusae* as an outgroup. Label values are given as BI/ML with values inferior to 0.7/70 replaced with a hyphen (-) and BI/ML values of 1/100 replaced with an asterisk (*), [T] indicates sequences derived from ex-type specimens or cultures.

Fig. S8. Phylogenetic tree of the best ML tree obtained using IQ-TREE of the *RPB2* gene dataset with selected species of *Nigrograna*, including *N. rubescens* in bold and *Occultibambusa bambusae* as an outgroup. Label values are given as BI/ML with values inferior to 0.7/70 replaced with a hyphen (-) and BI/ML values of 1/100 replaced with an asterisk (*), [T] indicates sequences derived from ex-type specimens or cultures.

Fig. S9. A. UPLC-HRMS extracted ion chromatogram (XIC) of *m/z* 323.1117 from the *Nigrograna rubescens* culture extract. The precursor protonated mass ion $[M+H]^+$ *m/z* of 323.1117 was observed to have two major chromatographic peaks associated at retention times of 3.85 min. (* major) and 4.27 min. (** minor). Observed HRMS/MS fragment ion and relative intensity values for *m/z* 323.1117 precursor ion occurring at: **B.** 3.85 min and **C.** 4.27 min.

Table S1. Primers and thermocycler cycles used for DNA amplification of the loci used during this study.

Table S2. GenBank accession number of newly generated sequences generated during this study and from strains used for the phylogenetic analyses.